

Enhancing the Mechanical Properties of Poly(vinyl alcohol) Fibers by Lithium Iodide Addition

Yusuke Taoka, Riza Asmaa Saari, Takumitsu Kida, Masayuki Yamaguchi, and Kazuaki Matsumura*

Cite This: *ACS Omega* 2023, 8, 32623–32634

Read Online

ACCESS |



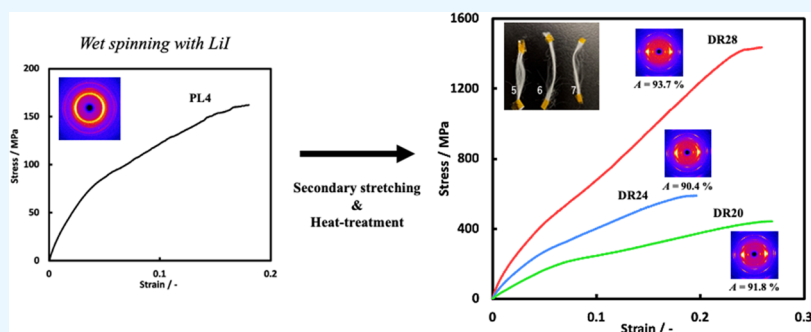
Metrics & More



Article Recommendations



Supporting Information



ABSTRACT: The effect of lithium iodide (LiI) on the mechanical strength, properties, and molecular orientation of poly(vinyl alcohol) (PVA) fibers spun by wet spinning and then heat-stretched was studied. The stretchability of LiI-PVA fibers was improved, and the rupture during stretching was suppressed compared to PVA fibers. In addition, the tensile strength and elastic modulus of the thermally stretched fibers have been significantly improved. It was also found that the addition of LiI improves the molecular orientation of PVA. This was achieved because LiI reduced the hydrogen bonds between the molecular chains of PVA, resulting in reduced crystallinity. Most of the LiI in the fiber could be removed by a coagulation bath and washing during the spinning process. This means that LiI is eventually removed, and the heat-treatment strengthens the hydrogen bonds, resulting in excellent mechanical strength.

INTRODUCTION

This paper reports on the effect of lithium iodide (LiI) on the mechanical strength and molecular orientation of poly(vinyl alcohol) (PVA) fibers. PVA is a water-soluble synthetic polymer with hydroxyl groups that exhibits chemical resistance, alkali resistance, biodegradability, and biocompatibility.^{1–5} It is suitable for various applications such as clothing, food packaging films, biomaterials, and fibers, and it is widely used in our daily lives.^{3,5–10} In particular, a PVA fiber is a highly effective material that can be used for infrastructure equipment that requires high reliability because it can be mass-produced at low cost and has high mechanical strength as a crystalline polymer.^{5,11–14} PVA fibers are used as cement reinforcement because they have good adhesion to cement matrices.^{5,13} Research to improve adhesion by modifying their surface has been conducted frequently in recent years.^{15,16}

However, PVA fiber is not the only high-performance fiber that has been developed in recent years. The textile industry has developed many high-performance fibers such as carbon fiber (CF), glass fiber (GF), and aramid fiber (AF).^{17–20} A great deal of research has been conducted on fiber-reinforced plastics (FRPs) with high strength and high modulus using these materials.^{21,22} These FRPs are used in many fields, including the automotive and aerospace industries, ships, and

infrastructure facilities, as an alternative to metals and ceramics due to their lightweight properties.^{20–24} However, CF and AF are very expensive, and GF has a weight problem. Moreover, these fibers have no established disposal method and can hardly be recycled.^{25–27} In view of current environmental issues, this is a major challenge that needs to be addressed. Therefore, this study aims to develop high-performance fibers with excellent mechanical properties, low cost, and low environmental impact by using lithium iodide (LiI) as an additive for PVA fibers.

Recently, some research has focused on the use of the PVA fiber as a reinforcing fiber in FRPs, and its low cost makes it a promising candidate.²⁸ In addition, the PVA fiber is extremely lightweight, making it excellent for FRPs. Nishikawa et al. mixed PVA fibers with polypropylene and molded them by injection molding.²⁹ They reported that this greatly improved the mechanical properties of polypropylene. This research

Received: May 11, 2023

Accepted: August 2, 2023

Published: August 31, 2023



shows promise for the application of the PVA fiber as a reinforcing fiber. Similar results have also been reported for composites of polypropylene and GF.³⁰ However, the use of GF increases weight. PVA fibers have lower mechanical properties than CF, however, comparable strength to GF can be achieved with perfect molecular orientation.^{28,29,31}

Many studies have attempted to increase the strength of PVA fibers, including syndiotactic poly(vinyl alcohol) (PVA with alternating stereochemistry).^{32–34} However, researchers have reported that orientation by advanced stretching is difficult for syndiotactic PVA because strong hydrogen bonds between PVA molecules inhibit high molecular orientation.³¹ Also, with the development of gel spinning and other methods, high-strength PVA fibers are available in the market. Many studies have been conducted on these fibers.^{35,36} However, these spinning methods use organic solvents and raise concerns about cost and environmental impact. Therefore, there are issues that need to be addressed. The PVA fiber was developed by Sakurada et al. using only water as a solvent. This method does not require acid or organic solvents for wet spinning and does not generate toxic gases in the production process.³⁷

Recently, Saari et al. added lithium bromide (LiBr), which improves the ductility of PVA fibers and increases their strength by reducing the hydrogen bonding network.²⁸ Similarly, they reported that adding LiI and LiBr to a PVA aqueous solution reduced hydrogen bonding in PVA more than LiBr alone.³⁸ This may result in a higher ductility enhancement effect than LiBr.

In this study, we added LiI to a PVA solution and spun fibers by a wet spinning method. Wet spinning is a fiber-forming process in which the polymer solution is extruded into a chemical bath that solidifies the filaments. We chose this method because it can produce fine and uniform fibers with high molecular orientation. We then heat-stretched the fibers at different temperatures and ratios and investigated how LiI affected their molecular orientation and mechanical properties.

EXPERIMENTAL SECTION

Materials. PVA was provided by Kuraray Co., Ltd (Tokyo, Japan). The degree of polymerization was 1700, and the degree of saponification was 99.8 mol %. LiI was purchased from Sigma-Aldrich (USA) and used without further purification. Sodium sulfate (Na_2SO_4) was purchased from Kanto Chemical Co., Ltd (Tokyo, Japan). Methanol was purchased from Nacalai Tesque (Kyoto, Japan). Distilled water was used throughout the experimental system.

Sample Preparation. The PVA solution was prepared by dissolving PVA in distilled water at 95 °C using a magnetic stirrer at a PVA concentration of 16 wt %. LiI was then added and stirred until the PVA was completely dissolved; the amount of LiI added was 0.1 molar ratio to the hydroxyl group of PVA. The amount of LiI added was determined according to the report by Saari et al.³⁸

PVA Fiber Spinning. Wet spinning was performed using a tabletop wet spinning machine (Nakamura Service Co., Ltd., Hokkaido, Japan). Figure 1 shows the schematic diagram of the spinning apparatus. A PVA/LiI solution was discharged from a solution tank kept at 90 °C into a coagulation bath filled with a saturated sodium sulfate solution. The diameter of the discharge nozzle was 0.2 mm. Primary stretching was performed at this stage, with a draw ratio (DR) of 4 for the fiber. After spinning, the fibers were washed with methanol,

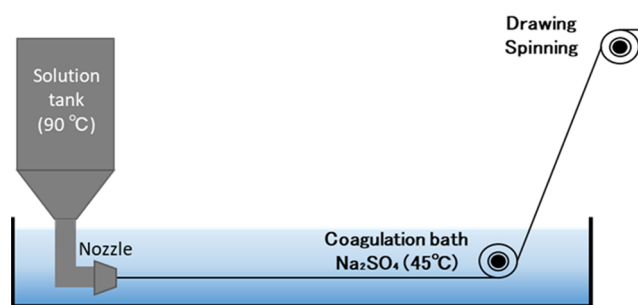


Figure 1. Schematic diagram of the wet spinning machine.

which does not dissolve PVA, to remove sodium sulfate and LiI. The fibers with nothing added were designated as pure PVA fibers, while the fibers with LiI added were designated as LiI-PVA fibers.

Secondary Stretching and Heat-treatment. Secondary stretching was performed by heat-stretching to improve the orientation and mechanical properties of PVA fibers using a tensile tester with a thermostatic chamber (Shimadzu Corporation Co., Ltd., Kyoto, Japan). After reaching the specified fiber temperature, the fiber was left to stand still for 2 min before stretching. The distance between the chucks was 10 mm. When stretching, the fibers were bundled and secured at both ends with polyimide tape. After stretching, the fiber was quenched by spraying it with ethanol and left in place for 1 min. The secondary extension multipliers were 4×, 5×, 6×, and 7×. The final drawing ratio was the combined ratio with the primary drawing ratio, which was 16×, 20×, 24×, and 28×. Heat treatment was then performed in order to induce crystallization. The respective conditions and sample names are summarized in Table 1. In the sample names, P4 indicates the pure PVA fiber with a primary stretch only; PL4 indicates the LiI-PVA fiber; P16 indicates the pure PVA fiber stretched 16×, and PL16 indicates the LiI-PVA fiber stretched 16×. For fibers stretched 20× or more, all fibers were spun with the addition of LiI. P20 indicates the draw ratio, 120–1.0 indicates the temperature and speed during heating and stretching, and the temperature of heat treatment is shown in parentheses. If the heat treatment is performed at 150 °C, there are two heat treatment time points indicated by –1 and –6 after the temperature in parentheses. To avoid the effects of moisture, the samples were stored in a vacuum desiccator because PVA is hygroscopic.

Measurements. Thermal analysis was performed by differential scanning calorimetry (DSC) to investigate the thermal transitions and crystallization behavior of PVA fibers (DSC6200, Seiko Instruments, Tokyo, Japan). About 10 mg of each sample was placed in an aluminum pan, sealed with a sealer, and measured under a nitrogen atmosphere at a temperature increase rate of 10 °C/min. An empty pan was used as the reference material. Samples were heated from 25 to 350 °C. Crystallinity X_C was calculated from the value of heat of fusion ΔH determined from the DSC heating curve using the following eq 1, where ΔH_f is the heat of fusion (152 J/g) in a perfect crystal of pure PVA.^{28,39}

$$X_C = \frac{\Delta H}{\Delta H_f} \times 100(\%) \quad (1)$$

The surface and shape of the spun PVA fibers were observed with a scanning electron microscope (SEM) (TM3030plus, Hitachi, Tokyo, Japan).

Table 1. Sample Name and Preparation Conditions

sample name	primary draw ratio	secondary draw ratio	draw ratio	drawing speed (mm/s)	drawing temperature (°C)	heat treatment
P4	4		4			90 °C one night
PL4			4			90 °C one night
P16		4	16	0.5	120	90 °C one night
PL16		4	16	0.5	120	90 °C one night
P20-120-1.0(120), P20-120-1.0(150)		5	20	1.0	120	120 °C
P24-120-1.0(120), P24-120-1.0(150)		6	24			one night, 150 °C 1 h
P28-120-1.0(120), P28-120-1.0(150)		7	28			
P20-180-1.0(120), P20-180-1.0(150)		5	20	1.0	180	120 °C
P24-180-1.0(120), P24-180-1.0(150)		6	24			one night, 150 °C 1 h
P28-180-1.0(120), P28-180-1.0(150)		7	28			
P20-180-1.5(120), P20-180-1.5(150-1)		5	20	1.5	180	120 °C
P24-180-1.5(120), P24-180-1.5(150-1)		6	24			one night, 150 °C 1 h
P28-180-1.5(120), P28-180-1.5(150-1)		7	28			
P20-180-1.5(150-6), P20-180-1.5(190)		5	20	1.5	180	150 °C 6 h, 190 °C 5 min
P24-180-1.5(150-6), P24-180-1.5(190)		6	24			
P28-180-1.5(150-6), P28-180-1.5(190)		7	28			

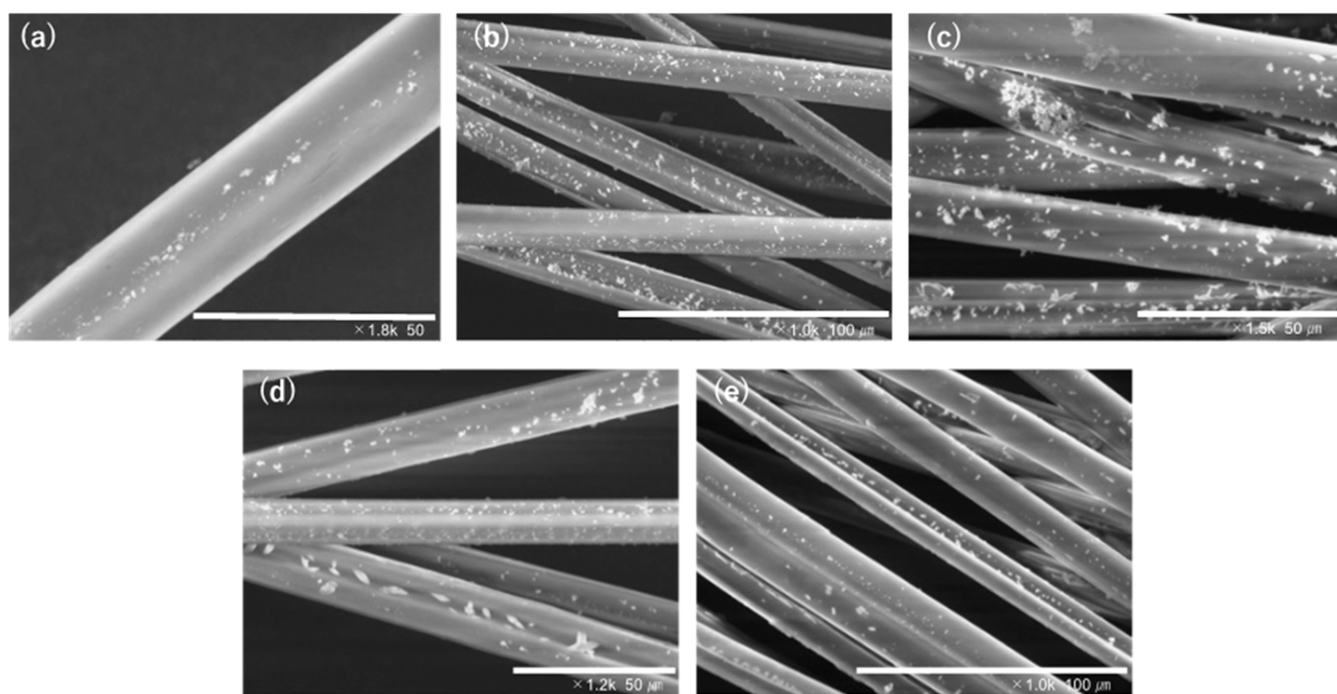


Figure 2. SEM images of PVA fibers. (a) Pure PVA DR16, (b) LiI-PVA DR16, (c) LiI-PVA DR20, (d) LiI-PVA DR24, and (e) LiI-PVA DR28.

Tensile tests were performed at room temperature using a tensile testing machine (Series 3360, Instron, USA) connected to a 5 N load cell. Each fiber was tested individually and fixed between chucks by fixing both ends to a sand paper. The distance between chucks was 12 mm, and the tensile speed was set at 0.2 mm/min. Three measurements were taken for each sample, and the average value was calculated.

Two-dimensional wide-angle X-ray diffraction (2D-WAXD) was measured using an X-ray diffractometer (XRD) (Smart Lab, Rigaku Corp., Tokyo, Japan) equipped with an imaging plate. 45 kV, 200 mA Cu K α radiation was applied to the fiber samples. The exposure time for each sample was 2700 seconds. The crystalline orientation of the PVA fiber was calculated and quantitatively evaluated by using the azimuthal distribution in the [101] plane. The orientation degree A was calculated by the half-width method using the following eq 2.²⁸

$$A = \frac{360 - \sum W_{\text{half}}}{360} \times 100 \quad (2)$$

where W_{half} is the half of the maximum value of the peak, i.e., the half-width.

Residual lithium concentrations were measured using the Metalloassay Lithium LS Kit (Metallogenics, Chiba, Japan), a lithium assay kit for measuring lithium concentrations in serum and plasma.⁴⁰ For the measurement, LiI-PVA solution was diluted to the specified value, PVA fiber solution, dissolved in hot water, and chromogenic solution were added to a 96-well plate. The absorbance was measured at 550 nm main wavelength and 600 nm secondary wavelength using a microplate reader (Infinito 200pro M Nano Plus, Tecan Japan, Kanagawa, Japan).

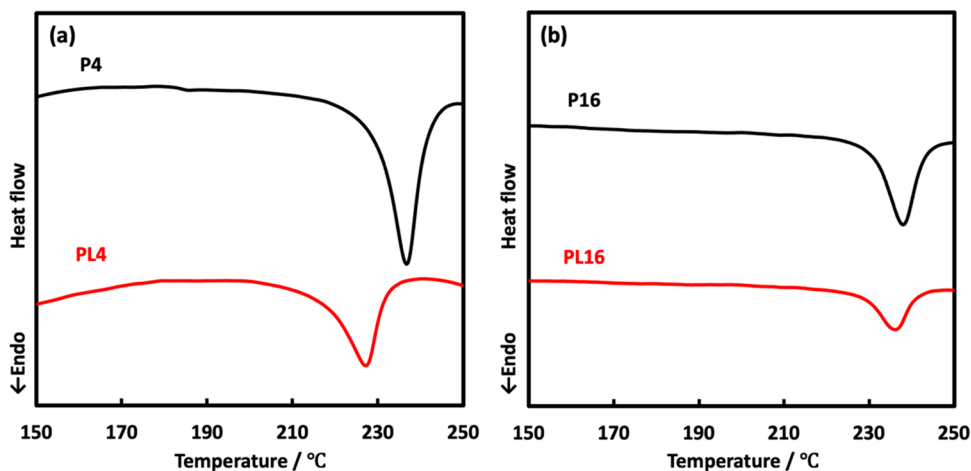


Figure 3. DSC heating curves of PVA fibers. (a) DR4 and (b) DR16.

RESULTS AND DISCUSSION

As shown in Figure 2, SEM images of PVA fibers revealed that there were white substances around the fiber, which were dried

Table 2. Melting Point and Crystallinity of Stretched PVA Fibers^a

	melting point (°C)	crystallinity (%)
P4	236 ± 0.2	36.2 ± 0.3
PL4	227 ± 0.1	28.3 ± 0.2
P16	236 ± 1.4	38.7 ± 1.9
PL16	233 ± 2.5	35.7 ± 0.9

^a(± standard error.)

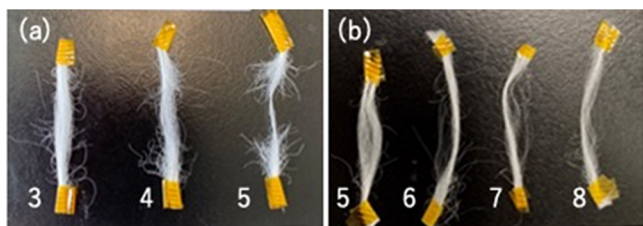


Figure 4. Heat-stretched PVA fibers. (a) Pure PVA and (b) LiI-PVA. The numbers alongside the fibers represent the drawing ratio for heat-stretching.

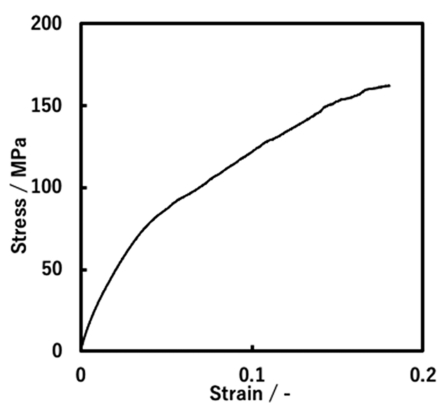


Figure 5. Stress–Strain curve of the nondrawing fiber (PL4).

sodium sulfate used in the spinning process to coagulate the polymer solution into solid fibers. The sodium sulfate solution

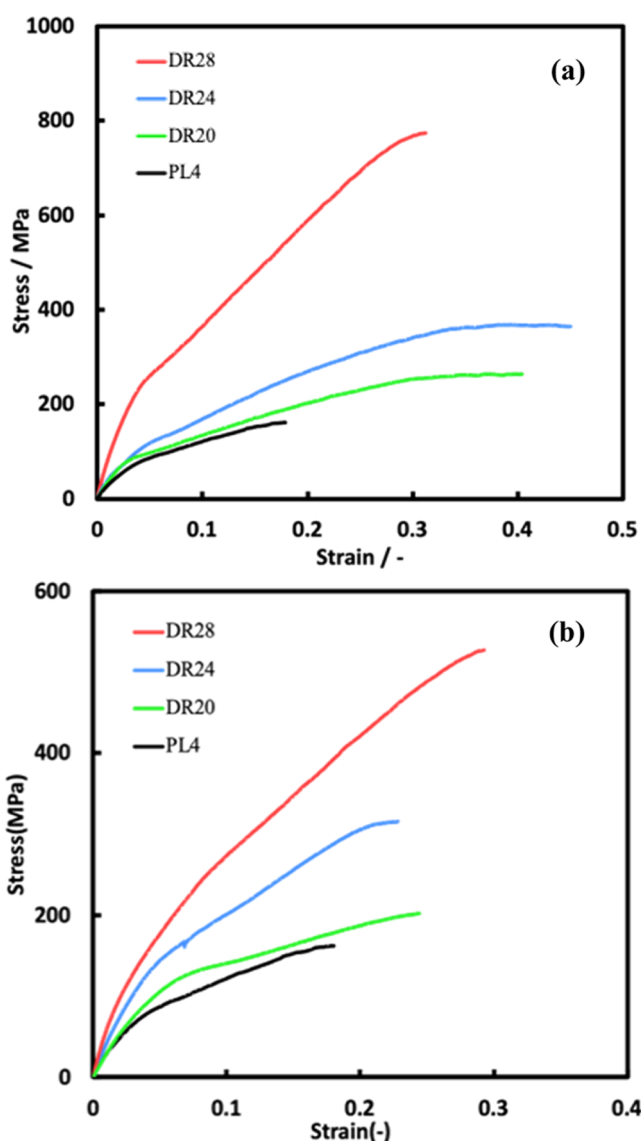


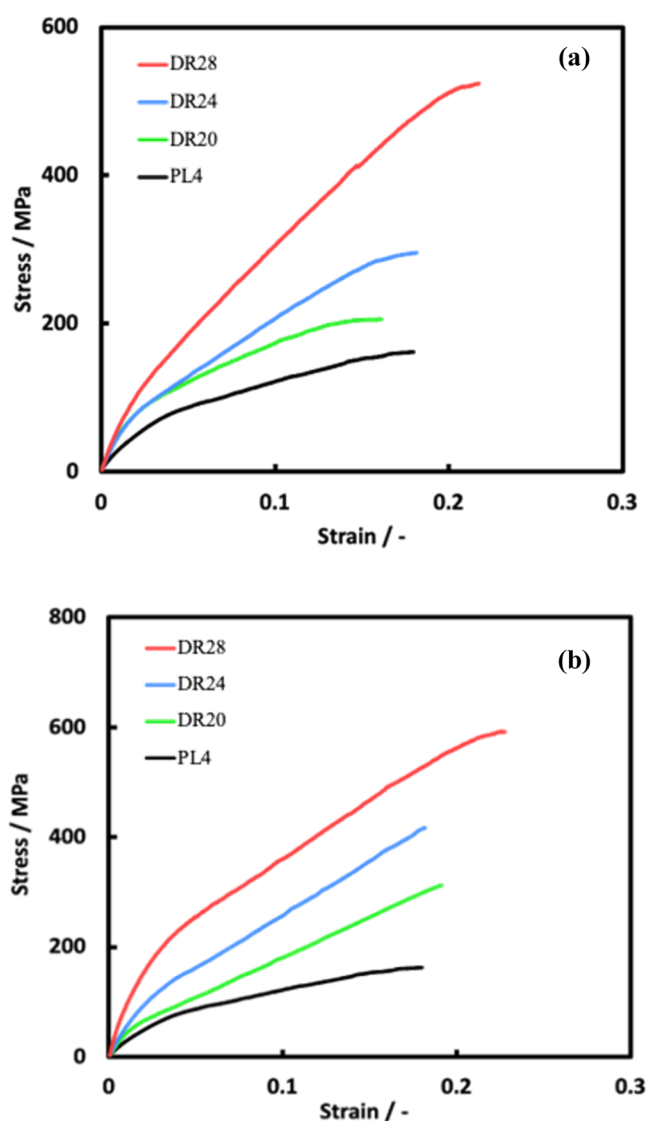
Figure 6. Stress–Strain curves of PVA fibers stretched at 120 °C, 1.0 mm/s. (a) Heat-treatment at 120 °C for one night and (b) heat-treatment at 150 °C for 1 h.

Table 3. Tensile Strength and Young's Modulus of Fibers Stretched at 120 °C, 1.0 mm/s^a

	tensile strength (MPa)	Young's modulus (GPa)
P20-120-1.0(120)	251 ± 13.4	3.5 ± 0.40
P24-120-1.0(120)	308 ± 38.4	4.1 ± 0.55
P28-120-1.0(120)	639 ± 67.9	9.7 ± 0.60
P20-120-1.0(150)	180 ± 21.6	3.0 ± 0.070
P24-120-1.0(150)	424 ± 62.0	5.9 ± 0.76
P28-120-1.0(150)	509 ± 44.5	5.4 ± 0.60

^a(± standard error.)**Table 4. Tensile Strength and Young's Modulus of Fibers Stretched at 180 °C, 1.0 mm/s^a**

	tensile strength (MPa)	Young's modulus (GPa)
P20-180-1.0(120)	176 ± 16.5	4.0 ± 0.43
P24-180-1.0(120)	246 ± 31.1	5.9 ± 0.39
P28-180-1.0(120)	370 ± 88.0	6.9 ± 0.90
P20-180-1.0(150)	242 ± 38.8	4.8 ± 0.43
P24-180-1.0(150)	309 ± 60.5	6.3 ± 0.10
P28-180-1.0(150)	460 ± 76.2	7.6 ± 2.0

^a(± standard error.)**Figure 7.** Stress–Strain curves of PVA fibers stretched at 180 °C, 1.0 mm/s. (a) Heat-treatment at 120 °C for one night and (b) heat-treatment at 150 °C for 1 h.

did not affect the physical properties of the fiber. The surface of the fiber was very smooth, indicating that no problem occurred during spinning. However, we observed that none of the PVA fibers were perfectly cylindrical in shape, which is a common phenomenon in wet spinning (Figure S1). In solution spinning methods such as wet spinning, the fiber shape depends on the solidification rate, which can vary depending on various factors such as temperature, concentration, and viscosity. Ideally, circularly shaped fibers have higher strength

than non-circular ones because they have less stress concentration and more uniform load distribution. Therefore, this shape irregularity was a problem not only for our study but also for other studies involving solution spinning of PVA and acrylic fibers.^{41,42} We calculated fiber diameters from SEM images and obtained average fiber diameters for each drawing ratio, DR16 [24.0 μm], DR20 [20.0 μm], DR24 [16.0 μm], and DR28 [13.0 μm] with small variation (Table S1).

As shown in Figure 3, the DSC heating curve of the PVA fiber reveals different melting peaks depending on the composition and stretching process. In P4, the melting peak appears at 236 °C, which is a characteristic peak of PVA due to its high degree of crystallization.⁴³ However, in PL4, the melting peak was reduced to 227 °C because LiI acts as a plasticizer that lowers the crystallization temperature and disrupts the hydrogen bonding network of PVA.²⁸ Figure 3b shows a PVA fiber after secondary stretching that had a higher melting point than that after only primary stretching. This indicates that secondary stretching increased the crystallinity and orientation of PVA fibers. The melting point measured from the DSC heating curve and the crystallinity X_C calculated using eq 1 are shown in Table 2.

This result is as expected and is caused by the fact that adding Li salts to PVA reduces crystallinity: Tretinnikov et al. reported that the addition of alkali metal salts to PVA changes crystallinity.⁴⁴ It has also been reported by Saari et al. that among alkali metal salts, lithium salts specifically decrease crystallinity.³⁸ It is known that the affinity between Li ions and hydroxyl groups (–OH) is high.⁴⁵ Therefore, the interaction of Li ions with the hydroxyl groups of PVA inhibits the hydrogen bonding between them, reducing its strength.

The effect of the Hofmeister series on PVA fibers was also investigated, as it has been reported to break hydrogen bonds and reduce crystallinity. Iodine ions, in particular, have a high hydrogen bond-breaking capacity,⁴⁶ which improves the crystallinity of the stretched fibers due to the stretching and heat generated during the process. The aim of the LiI addition is to suppress the hydrogen bonding during heating and dissolving, which results in defect-free orientation during spinning, and the subsequent removal of LiI, resulting in high-strength fibers. To induce crystallization, heat treatment was performed after secondary drawing, as it was found to be more effective than simultaneous heat treatment and drawing.

Figure 4 shows the drawn fibers at different draw ratios. In pure PVA, the number of broken fibers increased as the drawing ratio was increased, but in LiI-PVA, no fiber breakage was observed as the drawing ratio was increased. This indicates that the addition of LiI suppresses hydrogen bonding in PVA and reduces crystallinity, thereby improving the ductility of the PVA fiber. This phenomenon is a major discovery in the process of increasing the strength of PVA fibers during

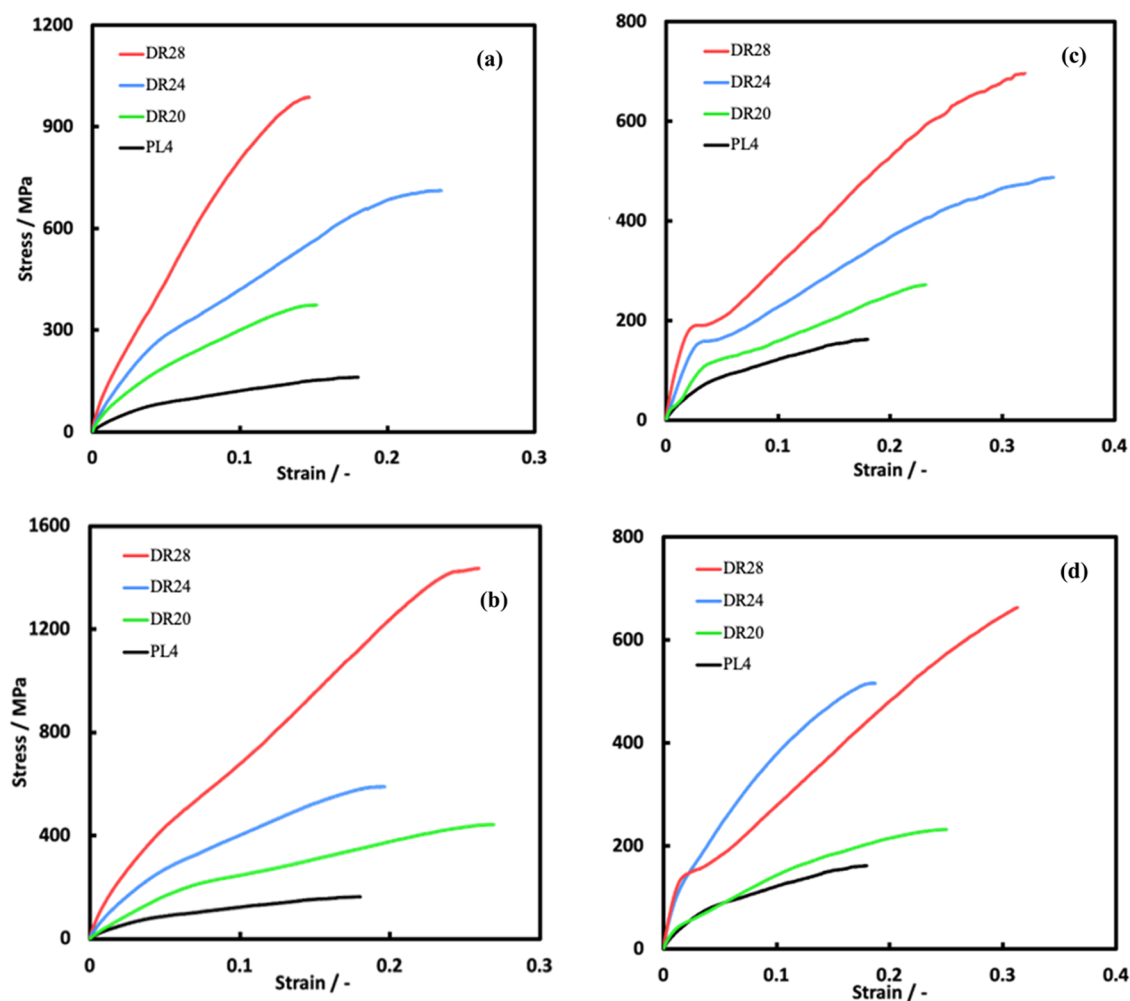


Figure 8. Stress–Strain curves of PVA fibers stretched at 180 °C, 1.5 mm/s. (a) Heat-treatment at 120 °C for one night, (b) heat-treatment at 150 °C for 1 h, (c) heat-treatment at 150 °C for 6 h, and (d) heat-treatment at 190 °C for 5 min.

Table 5. Tensile Strength and Young's Modulus of Fibers Stretched at 180 °C, 1.5 mm/s^a

	tensile strength (MPa)	Young's modulus (GPa)
P20-180-1.5(120)	316 ± 53.1	7.4 ± 0.50
P24-180-1.5(120)	588 ± 72.0	9.9 ± 0.41
P28-180-1.5(120)	842 ± 76.1	16 ± 0.39
P20-180-1.5(150)	352 ± 45.5	5.1 ± 0.36
P24-180-1.5(150)	519 ± 59.1	9.0 ± 0.76
P28-180-1.5(150)	1078 ± 232	16 ± 2.20
P20-180-1.5(150-6)	250 ± 12.8	5.1 ± 0.70
P24-180-1.5(150-6)	434 ± 18.4	6.2 ± 1.06
P28-180-1.5(150-6)	710 ± 27.3	11 ± 0.81
P20-180-1.5(190)	196 ± 36.0	3.2 ± 0.60
P24-180-1.5(190)	388 ± 68.3	6.7 ± 1.50
P28-180-1.5(190)	668 ± 18.4	9.6 ± 1.20

^a(± standard error.)

drawing. Previously, Saari et al. reported that the addition of LiBr to PVA and thermal drawing increased strength,²⁸ However, its drawing ratio was not very high. In this research, we have confirmed that heat-stretching can be performed up to 8X.

One characteristic of heat-stretching is its temperature dependence. At low temperatures, the material may break even

at a low drawing ratio when the stretching speed was increased. However, at high temperatures, the material could be stretched without a rupture even at a high drawing ratio. This behavior is likely due to the state of the molecular chains of PVA. For example, at lower temperatures, the molecular chains are less mobile, and the molecular chains slide, causing cleavage during stretching and orientation.^{47,48} In other words, higher temperatures increase the mobility of the molecular chains, thus preventing breakage during stretching. It has also been found that the temperature and speed during stretching affect the tensile strength and Young's modulus of PVA fibers.⁴⁴

The results of tensile testing of the fibers are shown. Stress–strain curves for each drawing and heat treatment condition are summarized. The values of the axes of stress in all graphs are unified. Nominal stress (in MPa) and nominal strain are also shown in these results.

Figure 5 shows the tensile test results for the fiber with only primary stretch (PL4), where PL4 donates the ratio of final to initial length during drawing. The tensile strength was found to 139 MPa, and its Young's modulus was 3.2 GPa, which is expected since no advanced stretching, involving additional heating and cooling cycles, was performed on the fiber. These results are being used as a reference point for comparison to results obtained from fibers that have undergone stretching.

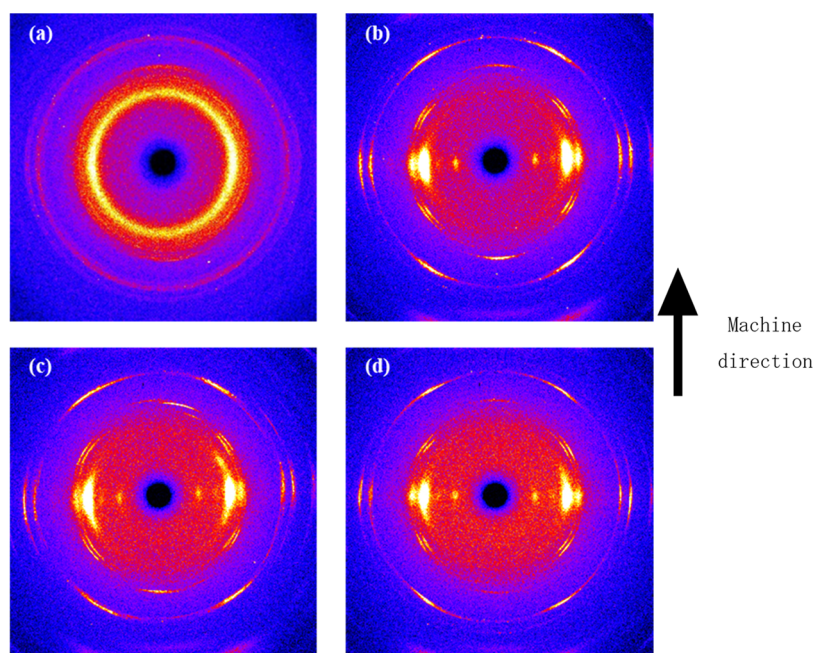


Figure 9. 2D-WAXD images of the PVA fiber stretched at 180 °C, 1.5 mm/s (the machine direction is in the direction of the arrow). (a) DR4, (b) DR20, (c) DR24, and (d) DR28.

Figure S2 shows the stress–strain curves for P16 and PL16. As can be seen, there is almost no difference between P16 and PL16 at 16 \times . The addition of LiI by itself does not indicate that it improves strength. However, by adding LiI, it is possible to achieve more than 16 \times stretched, which was not possible without lithium addition, as shown in Figure 4.

Figure 6 shows a representative nominal stress–nominal strain curve for a fiber drawn at 120 °C, 1.0 mm/s. Table 3 shows the average values and error ranges for tensile strength and Young's modulus. It is noteworthy that the differences in mechanical strength with a draw ratio (DR), which is the ratio of final to initial length during drawing, were substantial. Particularly for DR28, both the tensile strength and Young's modulus showed improvement compared to DR20. Furthermore, the fiber labeled as P28-120-1.0(120), which was stretched at 120 °C with DR28 and heat-treated at 120 °C, displayed the highest value of 775 MPa, serving as the champion data with an average value of 639 MPa. This indicates that secondary stretching, involving additional heating and cooling cycles after primary stretching, can enhance the strength of the fiber. It is worth noting that the effect of secondary stretching on fiber strength is likely influenced by the conditions of heat-treatment.

Figure 7 shows the results of the tensile test conducted on fibers stretched at 180 °C and 1.0 mm/s. Table 4 shows the average values and error ranges for the tensile strength and Young's modulus. The mechanical strength of these fibers was found to be lower than that of fibers stretched at 120 °C, 1.0 mm/s. Notably, when the heat-treatment condition was 120 °C for one night (24 h) (P28-180-1.0(120)), the average value was 370 MPa for DR28 and 524 MPa as champion data, which was lower than those obtained at other conditions. This may be due to the effect of higher temperature during stretching on the crystals of PVA, which are affected by heat exposure.^{5,49,50} Additionally, the decomposition of PVA can generate volatile products such as water, carboxyl acid, unsaturated aldehydes, and other unsaturated compounds.⁵¹

Figure 8 shows the results of tensile tests conducted on fibers stretched at 180 °C and 1.5 mm/s. Table 5 shows the average values and error ranges of the tensile strength and Young's modulus. The mechanical strength of fibers was found to be significantly improved by increasing the drawing speed while maintaining the stretching temperature at 180 °C. This improvement can be attributed to two factors. First, increasing the drawing speed reduced the exposure time of the fibers to high temperatures, preventing thermal decomposition. Second, high temperature and high drawing speed can suppress the relaxation of orientation during stretching, which is a common issue with stretched fibers. When fibers are stretched at high temperatures, the polymer molecular chain becomes more mobile and can easily be stretched in the direction of stress.⁴⁷ However, at high temperatures, the stretched molecular chains also become more mobile, and some degree of shrinkage occurs when the relaxation time of the molecular chains is long. This results in orientation relaxation, which reduces the fiber orientation, thereby decreasing strength and crystallinity.⁴⁷ As mentioned above, stretching speed is known to affect the mechanical strength of fibers, and it has been shown that fibers can attain very high mechanical strength at certain speeds.⁴⁷ Our study found that the highest value was obtained when the fibers were stretched at a relatively fast speed of 1.5 mm/s.

In addition to the differences observed in the mechanical strength of fibers under different drawing conditions, the study found that the heat-treatment conditions also have a significant impact on the fiber strength. For instance, the fiber heat-treated at 150 °C for 1 h (P28-180-1.5(150)) exhibited a tensile strength of 1436 MPa and Young's modulus of 18.9 GPa as champion data, which was about 1.5 times higher than the highest value obtained for other conditions. This finding is particularly interesting because heat-treatment is a crucial process used in many polymer products to improve their crystallinity, toughness, and water resistance.^{52,53} Thus, the results suggest that achieving high fiber strength requires

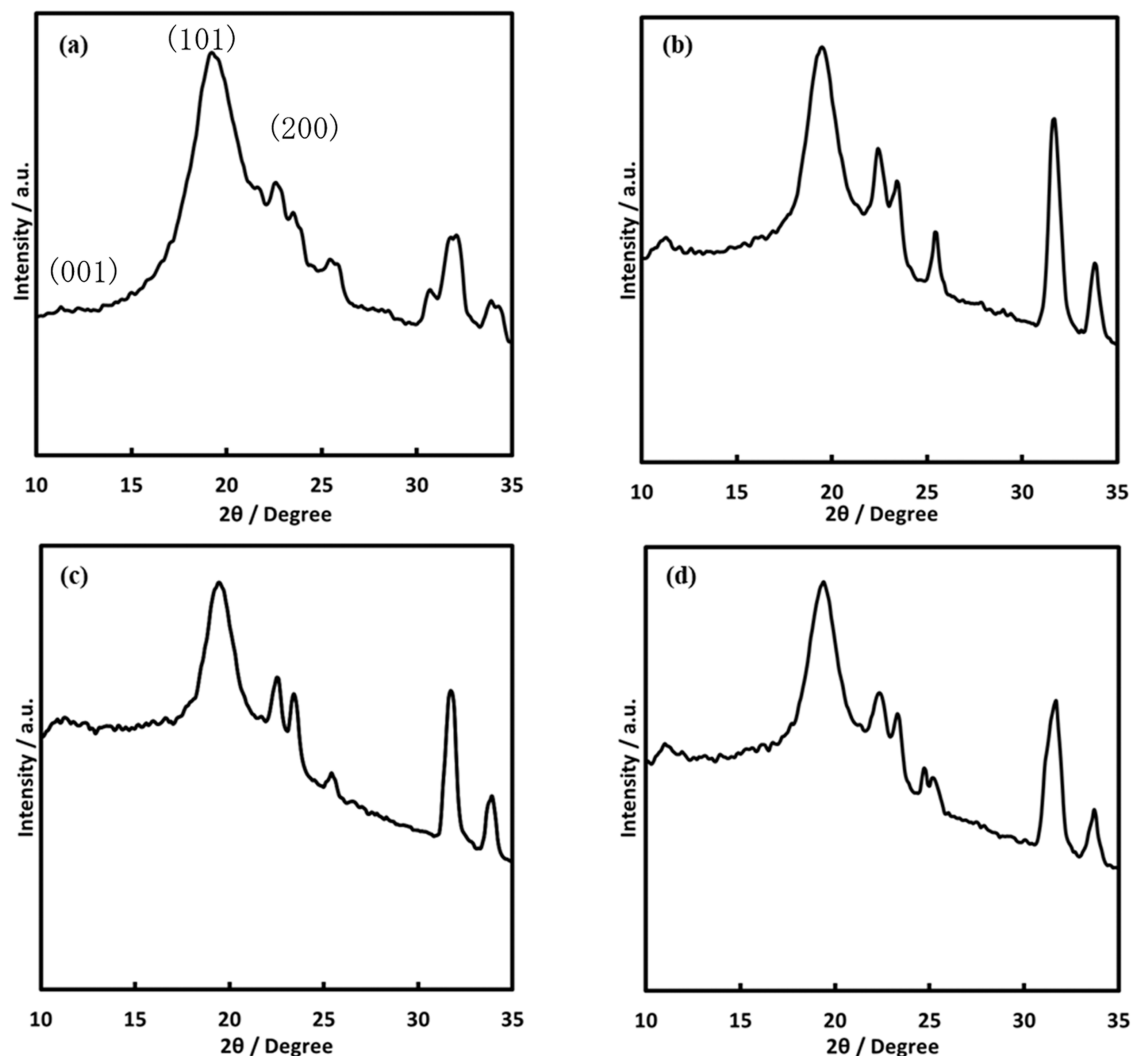


Figure 10. 2θ profile of PVA fibers stretched at 180 °C, 1.5 mm/s. (a) DR4, (b) DR20, (c) DR24, and (d) DR28.

optimizing not only the drawing conditions but also the heat-treatment conditions. Furthermore, the addition of LiI to suppress defects in molecular orientation during spinning alone may not be sufficient to achieve high fiber strength. Saari et al. reported that the drawing ratio of the LiBr-doped PVA fiber in their wet spinning method was about 10 \times , and its elastic modulus and tensile strength were 17.5 GPa and 177 MPa, respectively.²⁸ In our study, we were able to increase the drawing ratio by a factor of 28 \times , resulting in a significant increase in elastic modulus and tensile strength. This is attributed to the fact that LiI is more effective than LiBr in inhibiting hydrogen bonding, thereby reducing orientation defects during stretching.

Figures S3 and S4 present a comparison of the tensile strength and Young's modulus of fibers subjected to different drawing conditions. The fibers were stretched and heat-treated at either 1.0 or 1.5 mm/s at 180 °C. There is a large difference between the two drawing conditions. The numbers on the horizontal axis represent different samples. 'None' denotes fibers that were only subjected to primary stretching without any subsequent heat treatment. "1" denotes fibers that were stretched at 180 °C, 1.0 mm/s and heat-treated at 120 °C for one night. "2" denotes fibers that were stretched at 150 °C for 1 h. "3" denotes fibers that were stretched at 180 °C, 1.5 mm/s

and heat-treated at 120 °C for one night. "4" denotes fibers that were heat-treated at 150 °C for 1 h. "5" denotes fibers that were heat-treated at 150 °C for 6 h. "6" denotes fibers that were heat-treated at 190 °C for 5 min.

The crystalline orientation of the fibers subjected to the drawing and heat-treatment conditions that resulted in the highest strength was investigated using 2D-WAXD. Figure 9 displays 2D-WAXD images of unstretched and stretched fibers at 180 °C and 1.5 mm/s. In the X-ray diffraction images, the perpendicular direction is along the fiber axis. The stretched fiber exhibits strong diffraction spots at the equator, indicating that the molecular chains of PVA are oriented.

Figure 10 shows the 2θ profile at the equator. The profile exhibits α -monoclinic peaks in the (001), (101), and (200) crystal planes, which can be attributed to PVA. These peaks are easily identified since they have been previously reported in various studies.⁵⁴ The peak around 32–35° corresponds to sodium sulfate adhered to the fiber during spinning (Figures S5 and S6). This residue is left over from the washing process. As shown in Figure 9, the crystalline orientation of the PVA fiber is greatly enhanced by heat-stretching, and the (001), (101), and (200) equatorial spots, which are due to PVA crystals, are stronger than in the DR4 fiber. In particular, the equatorial spots are smaller for the DR28 fiber, indicating that

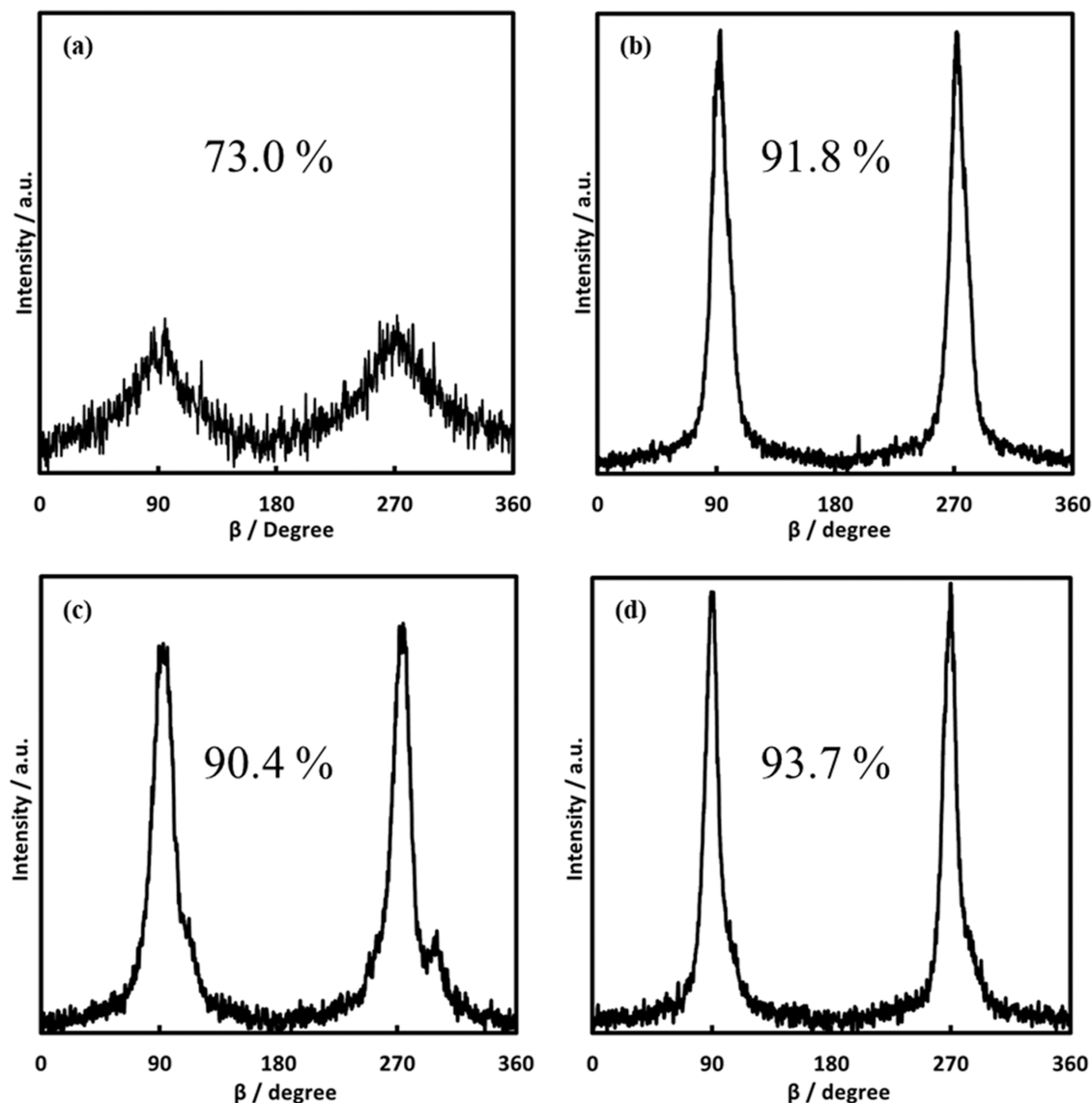


Figure 11. Azimuthal distribution in the (101) plane of A of PVA fibers stretched at 180 °C, 1.5 mm/s. (a) DR4, (b) DR20, (c) DR24, and (d) DR28.

Table 6. Measurements of Lithium Concentration^a

	lithium concentration (mg/mg)
LiI-PVA solution	0.30
fiber after spinning	0.05 ± 0.01
fibers after washing	0.01 ± 0.001

^a(± standard error.)

the crystalline orientation becomes stronger as the fiber is stretched and the draw ratio is increased.

Figure 11 illustrates the azimuthal distribution in the (101) crystal plane. The azimuthal distribution is used to determine the orientation of the molecular chains of PVA fibers.^{28,55} The widths of the peaks at values of β at 90° and 270° on the equator were evaluated. The diffraction patterns reveal a stronger orientation for fibers that have undergone secondary stretching, indicating that secondary stretching has enhanced the molecular orientation of PVA. Compared to DR4, the difference is significant, with an orientation value of 73.0%, which has now increased to over 90.0%. In particular, the highest value of 93.7% was achieved for DR28. This indicates

that it is possible to increase the orientation of the PVA fiber spun with LiI by stretching while applying heat. However, DR20 and DR24 did not show much difference in the degree of orientation. With DR28, the range of improvement became somewhat larger, and more advanced secondary stretching is required to increase the degree of orientation further. Although this study only evaluated PVA fibers stretched to a maximum of 28 \times , it was confirmed that it is possible to stretch PVA fibers to even higher stretch magnifications, which would improve the degree of orientation.

Residual LiI in the fiber can cause certain disadvantages for the industrial use of PVA fibers. The runoff of high concentrations of I, Br, and other halogens into the environment can harm ecosystems and nature.^{56,57} Additionally, several studies have been conducted on the risks of plasticizers in polymer products.^{58–60} This means that care should be taken regarding additives and plasticizers in polymer products. Therefore, we investigated the residual Li concentration.

Table 6 displays the Li concentration in the LiI-PVA solution before spinning, the fiber after spinning, and the fiber after washing. The Li concentration in the final PVA fiber was 0.01 mg/mg. The Li ion concentration of the LiI-added PVA solution used for spinning was 0.30 mg/mg. In other words, it was found that about 97% of the lithium was removed compared to the amount of lithium in the solution state. This indicates that most of the LiI can be removed by wet spinning and washing. Therefore, PVA fibers produced by this method can be used in many fields without any issues.

In this study, we focused on increasing strength by improving ductility and orientation. Although a significant improvement in mechanical strength was confirmed, there were limitations with the current method, such as the variability caused by manual wet spinning. However, we found that stretching of 28× or more was possible, and the improvement in stretchability due to the addition of LiI was tremendous. It was not possible to obtain the mechanical strength of high-performance fibers such as CF and GF. However, our proposed wet spinning of the LiI-based PVA fiber can be easily mass-produced using current equipment. This can minimize the cost increase in industrial applications to the greatest extent possible. In addition, wet spinning of the PVA fiber is an organic solvent-free method with a low environmental impact, which is one of the solutions to our current environmental problems.

In the future, we believe that further improvement of mechanical strength and molecular orientation can be achieved by using mechanically spinnable equipment to enable uniform stretching. Furthermore, the interfacial strength of PVA fibers with a matrix resin as FRP reinforcing fibers should be evaluated.

CONCLUSIONS

In this study, we proposed a new method for producing high-strength PVA fibers for composite applications by adding LiI to reduce hydrogen bonds in the PVA molecular chain and improve the spinnability of the PVA fibers. We enhanced the mechanical strength of the PVA fibers by improving their heat stretchability and increasing their level of molecular orientation. We were able to remove almost all of the LiI added to PVA through the spinning and washing processes. This simple and effective method of increasing the strength of PVA fibers can be achieved by simply adding LiI to the PVA solution, which is the raw material for spinning. This technology has the potential to provide inexpensive, lightweight, and mechanically strong PVA fibers that can contribute to the development of high sustainability.

ASSOCIATED CONTENT

Data Availability Statement

The experimental data that support the findings of this study are available from the corresponding author upon reasonable request.

Supporting Information

The Supporting Information is available free of charge at <https://pubs.acs.org/doi/10.1021/acsomega.3c03280>.

Fiber diameter data, SEM image of fibers, tensile strength and Young's modulus of fibers stretched at various conditions, and XRD profile of PVA films (PDF)

AUTHOR INFORMATION

Corresponding Author

Kazuaki Matsumura – School of Materials Science, Japan Advanced Institute of Science and Technology, Nomi, Ishikawa 923-1211, Japan; orcid.org/0000-0001-9484-3073; Email: mkazuaki@jaist.ac.jp

Authors

Yusuke Taoka – School of Materials Science, Japan Advanced Institute of Science and Technology, Nomi, Ishikawa 923-1211, Japan

Riza Asmaa Saari – School of Materials Science, Japan Advanced Institute of Science and Technology, Nomi, Ishikawa 923-1211, Japan

Takumitsu Kida – School of Materials Science, Japan Advanced Institute of Science and Technology, Nomi, Ishikawa 923-1211, Japan

Masayuki Yamaguchi – School of Materials Science, Japan Advanced Institute of Science and Technology, Nomi, Ishikawa 923-1211, Japan; orcid.org/0000-0002-7640-3768

Complete contact information is available at:

<https://pubs.acs.org/10.1021/acsomega.3c03280>

Notes

The authors declare no competing financial interest.

ACKNOWLEDGMENTS

This study was supported by JST COI program “Construction of next-generation infrastructure systems using innovative materials— Realization of a safe and secure society that can coexist with the Earth for centuries.”

REFERENCES

- (1) Baker, M. I.; Walsh, S. P.; Schwartz, Z.; Boyan, B. D. A review of polyvinyl alcohol and its uses in cartilage and orthopedic applications. *J. Biomed. Mater. Res., Part B* **2012**, *100*, 1451–1457.
- (2) Kawai, F.; Hu, X. Biochemistry of microbial polyvinyl alcohol degradation. *Appl. Microbiol. Biotechnol.* **2009**, *84*, 227–237.
- (3) Demerlis, C. C.; Schoneker, D. R. Review of the oral toxicity of polyvinyl alcohol (PVA). *Food Chem. Toxicol.* **2003**, *41*, 319–326.
- (4) Shima, M. Biodegradation of plastics. *Curr. Opin. Biotechnol.* **2001**, *12*, 242–247.
- (5) Slam, M.; Kalyar, M. A.; Raza, Z. A. Polyvinyl alcohol: A review of research status and use of polyvinyl alcohol based nanocomposites. *Polym. Eng. Sci.* **2018**, *58*, 119–2132.
- (6) Gaikwad, K. K.; Lee, J. Y.; Lee, Y. S. Development of polyvinyl alcohol and apple pomace bio-composite film with antioxidant properties for active food packaging application. *J. Food Sci. Technol.* **2016**, *53*, 1608–1619.
- (7) Kanatt, S. R.; Rao, M. S.; Chawla, S. P.; Sharma, A. Active chitosan-polyvinyl alcohol films with natural extracts. *Food Hydrocolloids* **2012**, *29*, 290–297.
- (8) Matsumura, K. Special issue: Nanocomposite hydrogels for biomedical applications. *Appl. Sci.* **2020**, *10*, 389.
- (9) Sakaguchi, T.; Nagano, S.; Hara, M.; Hyon, S. H.; Patel, M.; Matsumura, K. Facile preparation of transparent poly(vinyl alcohol) hydrogels with uniform microcrystalline structure by hot-pressing without using organic solvents. *Polym. J.* **2017**, *49*, 535–542.
- (10) Zhao, Y.; Terai, W.; Hoshijima, Y.; Gotoh, K.; Matsuura, K.; Matsumura, K. Development and characterization of a poly(Vinyl Alcohol)/graphene oxide composite hydrogel as an artificial cartilage material. *Appl. Sci.* **2018**, *8*, 2272.

- (11) Si, W.; Cao, M.; Li, L. Establishment of fiber factor for rheological and mechanical performance of polyvinyl alcohol (PVA) fiber reinforced mortar. *Constr. Build. Mater.* **2020**, *265*, No. 120347.
- (12) Nam, J.; Kim, G.; Lee, B.; Hasegawa, R.; Hama, Y. Frost resistance of polyvinyl alcohol fiber and polypropylene fiber reinforced cementitious composites under freeze thaw cycling. *Composites, Part B* **2016**, *90*, 241–250.
- (13) Thong, C. C.; Teo, D. C. L.; Ng, C. K. Application of polyvinyl alcohol (PVA) in cement-based composite materials: A review of its engineering properties and microstructure behavior. *Constr. Build. Mater.* **2016**, *107*, 172–180.
- (14) Jang, J.; Lee, D. K. Plasticizer effect on the melting and crystallization behavior of polyvinyl alcohol. *Polymer* **2003**, *44*, 8139–8146.
- (15) Zhang, W.; Zou, X.; Wei, F.; Wang, H.; Zhang, G.; Huang, Y.; Zhang, Y. Grafting SiO₂ nanoparticles on polyvinyl alcohol fibers to enhance the interfacial bonding strength with cement. *Composites, Part B* **2019**, *162*, 500–507.
- (16) Curosu, I.; Liebscher, M.; Alsous, G.; Muja, E.; Li, H.; Drechsler, A.; Frenzel, R.; Synytska, A.; Mechtcherine, V. Tailoring the crack-bridging behavior of strain-hardening cement-based composites (SHCC) by chemical surface modification of poly(vinyl alcohol) (PVA) fibers. *Cem. Concr. Compos.* **2020**, *114*, No. 103722.
- (17) Huang, X. Fabrication and properties of carbon fibers. *Materials* **2009**, *2*, 2369–2403.
- (18) Chen, J.; Zhao, D.; Jin, X.; Wang, C.; Wang, D.; Ge, H. Modifying glass fibers with graphene oxide: Towards high-performance polymer composites. *Compos. Sci. Technol.* **2014**, *97*, 41–45.
- (19) Gore, P. M.; Kandasubramanian, B. Functionalized Aramid Fibers and Composites for Protective Applications: A Review. *Ind. Eng. Chem. Res.* **2018**, *57*, 16537–16563.
- (20) Zhang, B.; Jia, L.; Tian, M.; Ning, N.; Zhang, L.; Wang, W. Surface and interface modification of aramid fiber and its reinforcement for polymer composites: A review. *Eur. Polym. J.* **2021**, *147*, No. 110352.
- (21) Prashanth, S.; Subbaya, K. M.; Nithin, K.; Sachhidananda, S. Fiber Reinforced Composites—A Review. *Mater. Sci. Eng.* **2017**, *6*, No. 1000341.
- (22) Rubino, F.; Nisticò, A.; Tucci, F.; Carlone, P. Marine application of fiber reinforced composites: A review. *J. Mar. Sci. Eng.* **2020**, *8*, 26.
- (23) Hegde, S.; Satish Shenoy, B.; Chethan, K. N. Review on carbon fiber reinforced polymer (CFRP) and their mechanical performance. *Mater. Today: Proc.* **2019**, *19*, 658–662.
- (24) Ahmad, H.; Markina, A. A.; Porotnikov, M. V.; Ahmad, F. A review of carbon fiber materials in automotive industry. *IOP Conf. Ser.: Mater. Sci. Eng.* **2020**, *971*, No. 032011.
- (25) Jacob, A. Composites can be recycled. *Reinf. Plast.* **2011**, *55*, 45–46.
- (26) Cousins, D. S.; Suzuki, Y.; Murray, R. E.; Samaniuk, J. R.; Stebner, A. P. Recycling glass fiber thermoplastic composites from wind turbine blades. *J. Cleaner Prod.* **2019**, *209*, 1252–1263.
- (27) Naqvi, S. R.; Prabhakara, H. M.; Bramer, E. A.; Dierkes, W.; Akkerman, R.; Brem, G. A critical review on recycling of end-of-life carbon fibre/glass fibre reinforced composites waste using pyrolysis towards a circular economy. *Resour., Conserv. Recycl.* **2018**, *136*, 118–129.
- (28) Saari, R. A.; Maeno, R.; Marujiwat, W.; Nasri, M. S.; Matsumura, K.; Yamaguchi, M. Modification of poly(vinyl alcohol) fibers with lithium bromide. *Polymer* **2021**, *213*, No. 123193.
- (29) Nishikawa, R.; Aridome, N.; Ojima, N.; Yamaguchi, M. Structure and properties of fiber-reinforced polypropylene prepared by direct incorporation of aqueous solution of poly(vinyl alcohol). *Polymer* **2020**, *199*, No. 122566.
- (30) Guo, M.; Yang, H.; Tan, H.; Wang, C.; Zhang, Q.; Du, R.; Fu, Q. Shear enhanced fiber orientation and adhesion in PP/glass fiber composites. *Macromol. Mater. Eng.* **2006**, *291*, 239–246.
- (31) Lai, D.; Wei, Y.; Zou, L.; Xu, Y.; Lu, H. Wet spinning of PVA composite fibers with a large fraction of multi-walled carbon nanotubes. *Prog. Nat. Sci.* **2015**, *25*, 445–452.
- (32) Nagashima, N.; Matsuzawa, S.; Okazaki, M. Syndiotacticity-rich poly(vinyl alcohol) fibers spun from N-methylmorpholine-N-oxide/water mixture. *J. Appl. Polym. Sci.* **1996**, *62*, 1551–1559.
- (33) Wang, H.; He, J.; Zou, L.; Wang, C.; Wang, Y. Synthesis of syndiotacticity-rich high polymerization degree PVA polymers with VAc and VP_a, fabrication of PVA fibers with superior mechanical properties by wet spinning. *J. Polym. Res.* **2021**, *28*, 386.
- (34) Dai, L.; Ying, L. Infrared Spectroscopic Investigation of Hydrogen Bonding in EVOH Containing PVA Fibers. *Macromol. Mater. Eng.* **2002**, *287*, 509–514.
- (35) Hong, X.; Xu, Y.; Zou, L.; Li, Y. V.; He, J.; Zhao, J. The Effect of Degree of Polymerization on the Structure and Properties of Polyvinyl Alcohol Fibers with High Strength and High Modulus. *J. Appl. Polym. Sci.* **2021**, *138*, 49971.
- (36) Hong, X.; He, J.; Zou, L.; Wang, Y.; Li, Y. V. Preparation and Characterization of High Strength and High Modulus PVA Fiber via Dry-wet Spinning with Cross-linking of Boric Acid. *J. Appl. Polym. Sci.* **2021**, *138*, 51394.
- (37) Sakurada, I. Wet Spinning I: Use of a Sodium Bath. In *Poly(vinyl alcohol) Fibers*; Sakurada, I., Ed.; Maecel Dekker. Inc.: New York and Basel, 1985; pp 63–186.
- (38) Saari, R. A.; Maeno, R.; Tsuyuguchi, R.; Marujiwat, W.; Phulkerd, P.; Yamaguchi, M. Impact of Lithium halides on rheological properties of aqueous solution of poly (vinyl alcohol). *J. Polym. Res.* **2020**, *27*, 218.
- (39) Wang, X.; Park, S. Y.; Yoon, K. H.; Lyoo, W. S.; Min, B. G. The effect of multi-walled carbon nanotubes on the molecular orientation of poly(vinyl alcohol) in drawn composite films. *Fibers Polym.* **2006**, *7*, 323–327.
- (40) Iwai, M.; Kondo, F.; Suzuki, T.; Ogawa, T.; Seno, H. Application of Lithium Assay kit LS for quantification of lithium in whole blood and urine. *Leg. Med.* **2021**, *49*, No. 101834.
- (41) Tsai, J. S.; Su, W. C. Control of cross-section shape for polyacrylonitrile fibre during wet-spinning. *J. Mater. Sci. Lett.* **1991**, *10*, 1253–1256.
- (42) Wang, Y. X.; Wang, C. G.; Yu, M. J. Effects of different coagulation conditions on polyacrylonitrile fibers wet spun in a system of dimethylsulphoxide and water. *J. Appl. Polym. Sci.* **2007**, *104*, 3723–3729.
- (43) Thomas, D.; Cebe, P. Self-nucleation and crystallization of polyvinyl alcohol. *J. Therm. Anal. Calorim.* **2017**, *127*, 885–894.
- (44) Tretinnikov, O. N.; Zagorskaya, S. A. Effect of alkali halide salt additives on the structure of poly(vinyl alcohol) films cast from aqueous solutions. *Polym. Sci., Ser. A* **2013**, *55*, 463–470.
- (45) Ma, N. L.; Siu, F. M.; Tsang, C. W. Interaction of alkali metal cations and short chain alcohols: effect of core size on theoretical affinities. *Chem. Phys. Lett.* **2000**, *322*, 65–72.
- (46) Saari, R. A.; Nasri, M. S.; Marujiwat, W.; Maeno, R.; Yamaguchi, M. Application of the Hofmeister series to the structure and properties of poly(vinyl alcohol) films containing metal salts. *Polym. J.* **2021**, *53*, 557–564.
- (47) Wu, Q.; Chen, N.; Wang, Q. Crystallization behavior of melt-spun poly(vinyl alcohol) fibers during drawing process. *J. Polym. Res.* **2010**, *17*, 903–909.
- (48) Salem, D. R. Crystallization kinetics during hot-drawing of poly(ethylene terephthalate) film: strain-rate/draw-time superposition. *Polymer* **1992**, *33*, 3189–3192.
- (49) Voronova, M. I.; Surov, O. V.; Guseinov, S. S.; Barannikov, V. P.; Zakharov, A. G. Thermal stability of polyvinyl alcohol/nano-crystalline cellulose composites. *Carbohydr. Polym.* **2015**, *130*, 440–447.
- (50) Wu, W.; Tian, H.; Xiang, A. Influence of Polyol Plasticizers on the Properties of Polyvinyl Alcohol Films Fabricated by Melt Processing. *J. Polym. Environ.* **2012**, *20*, 63–69.

(51) Lu, R.; Ma, E.; Xu, Z. Application of pyrolysis process to remove and recover liquid crystal and films from waste liquid crystal display glass. *J. Hazard. Mater.* **2012**, *243*, 311–318.

(52) Simmons, H.; Tiwary, P.; Colwell, J. E.; Kontopoulou, M. Improvements in the crystallinity and mechanical properties of PLA by nucleation and annealing. *Polym. Degrad. Stab.* **2019**, *166*, 248–257.

(53) Schrauwen, B. A. G.; Janssen, R. P. M.; Govaert, L. E.; Meijer, H. E. H. Intrinsic deformation behavior of semicrystalline polymers. *Macromolecules* **2004**, *37*, 6069–6078.

(54) Minus, M. L.; Chae, H. G.; Kumar, S. Single wall carbon nanotube templated oriented crystallization of poly(vinyl alcohol). *Polymer* **2006**, *47*, 3705–3710.

(55) Hong, X.; Xu, Y.; Zou, L.; Li, Y. V.; He, J.; Zhao, J. The effect of degree of polymerization on the structure and properties of polyvinyl alcohol fibers with high strength and high modulus. *J. Appl. Polym. Sci.* **2021**, *138*, 49971.

(56) Harkness, J. S.; Dwyer, G. S.; Warner, N. R.; Parker, K. M.; Mitch, W. A.; Vengosh, A. Iodide, bromide, and ammonium in hydraulic fracturing and oil and gas wastewaters: Environmental implications. *Environ. Sci. Technol.* **2015**, *49*, 1955–1963.

(57) Watson, K.; Farré, M. J.; Knight, N. Strategies for the removal of halides from drinking water sources, and their applicability in disinfection by-product minimisation: A critical review. *J. Environ. Manage.* **2012**, *110*, 276–298.

(58) Halden, R. U. Plastics and health risks. *Annu. Rev. Public Health* **2010**, *31*, 179–194.

(59) Gustafsson, E.; Bowden, T. M.; Rennie, A. R. Interactions of amphiphiles with plasticisers used in polymers: Understanding the basis of health and environmental challenges. *Adv. Colloid Interface Sci.* **2020**, *277*, No. 102109.

(60) Mukhopadhyay, M.; Jalal, M.; Vignesh, G.; Ziauddin, M.; Sampath, S.; Bharat, G. K.; Nizzetto, L.; Chakraborty, P. Migration of Plasticizers from Polyethylene Terephthalate and Low-Density Polyethylene Casing into Bottled Water: A Case Study From India. *Bull. Environ. Contam. Toxicol.* **2022**, *109*, 949–955.